J. Cent. South Univ. (2024) 31: 1092−1106
DOI: https://doi.org/10.1007/s11771-024-5639-y

Springer

Contaminant transport modelling of heavy metal pollutants in soil and groundwater: An example at a non-ferrous smelter site

ZHANG Hai-li(张海丽)[1, 2], ZHAO Peng(赵鹏)[1, 2], GAO Wen-yan(高文艳)[3],
XIAO Bao-hua(肖保华)[1], YANG Xue-feng(杨雪枫)[1, 2], SONG Lei(宋磊)[1, 2],
FENG Xiang(冯翔)[4], GUO Lin(郭林)[4], LU Yong-ping(陆永平)[5], LI Hai-feng(李海峰)[5], SUN Jing(孙静)[1]*

1. State Key Laboratory of Environmental Geochemistry, Institute of Geochemistry, Chinese Academy of Sciences, Guiyang 550081, China;
2. College of Earth and Planetary Sciences, University of Chinese Academy of Sciences, Beijing 101408, China;
3. School of Metallurgy and Environment, Central South University, Changsha 410083, China;
4. Henan Academy of Geology, Zhengzhou 450001, China;
5. China Railway Seventh Bureau Group Nanjing Engineering Co., Ltd., Nanjing 210000, China

Abstract: The topsoil of smelter sites is subjected to severe contamination by heavy metals (HMs). Existing numerical simulations typically treat soil and groundwater separately owing to data limitations and computational constraints, which does not reflect the actual situation. Herein, a three-dimensional coupled soil-groundwater reactive solute transport numerical model was developed using the Galerkin finite element method with the smelter as the research object. This model treats soil and groundwater as a whole system, providing a quantitative characterization of HMs migration patterns in soil and groundwater. The model used the reaction coefficient (λ) and retention coefficient (R) to describe the release and adsorption capacities of HMs. Results from the model were consistent with actual pollution distributions in the field, indicating the efficacy of the soil-groundwater remediation technology for severe soil and localized groundwater pollution. The constructed three-dimensional coupled soil-groundwater reactive solute transport model can describe and predict the distribution and transport diffusion behavior of HMs at the study site with good efficacy. The model was also used to simulate and predict the effects of remediation technologies during the treatment of smelting site contamination, providing guidance for optimizing the treatment plan.

Key words: non-ferrous smelting sites; heavy metal pollution; transportation and transformation mechanisms; diffusion flux prediction; remediation technology simulation

Cite this article as: ZHANG Hai-li, ZHAO Peng, GAO Wen-yan, XIAO Bao-hua, YANG Xue-feng, SONG Lei, FENG Xiang, GUO Lin, LU Yong-ping, LI Hai-feng, SUN Jing. Contaminant transport modelling of heavy metal pollutants in soil and groundwater: An example at a non-ferrous smelter site [J]. Journal of Central South University, 2024, 31(4): 1092−1106. DOI: https://doi.org/10.1007/s11771-024-5639-y.

Foundation item: Project(2019YFC1803601) supported by the National Key Research and Development Program of China; Project(GCC [2023]038) supported by Guizhou "Hundred" High-level Innovative Talent Project, China
Received date: 2023-12-25; **Accepted date:** 2024-04-20
Corresponding author: SUN Jing, PhD, Professor; E-mail: sunjing@mail.gyig.ac.cn; ORCID: https://orcid.org/0000-0002-0129-5184

1 Introduction

The rapid development of industrial activities has led to a substantial rise in soil-groundwater heavy metals (HMs) contamination in recent years. Nonferrous smelting activities, which cause HMs pollution, contamination from solid waste accumulation, and other environmental hazards, are among the most important sources of toxic metals in soil [1]. Soil-groundwater contamination stems from long-term filtration and leaching of solid wastes and contaminated soil through rainfall, releasing large amounts of Cd, Cu, Pb, Zn, and other HMs into the surrounding environment through surface runoff and groundwater migration. Consequently, this poses severe health risks to humans [2, 3]. Studies have shown extremely high concentrations of hazardous HMs such as Cd, Ni, Cu, Pb, Zn, As and Hg in contaminated smelting sites worldwide [4]. These HMs exhibit characteristics such as intractability, accumulation, toxicity, invisibility, long-term effects, and irreversibility, posing serious threats to the surrounding environment and human health.

Researchers are currently focusing on soil HM contamination in terms of contamination sources, the spatial distribution of HMs, and their chemical forms within the soil [5]. Once exogenous HMs enter the soil, a series of environmental processes occur at the solid-liquid interface [6]. Soil hosts a dynamic adsorption-desorption equilibrium process for cations and anions of HMs, with their reaction behavior dictating migration ability and bioavailability of HMs [7]. The adsorption of HMs by various minerals and soil types has been studied in single-metal systems [8]. Numerous studies have also been conducted to understand competitive adsorption of trace elements in pure minerals, organic compounds, and acidic soils [9, 10]. Findings indicate that the main physical and chemical factors controlling adsorption are not solely dependent on their contents in soil but also on soil characteristics, HMs properties, and environmental factors [11]. Moreover, the presence of other metals can influence the adsorption-desorption behavior of metals within the soil matrix. Much researches have scrutinized HMs concerning their soil accumulation, plant uptake, and groundwater contamination. However, research on simulating the HM adsorption within complex, multielement systems such as soil is limited, and their competitive adsorption in soil and the resultant environmental transport capacities of HMs are poorly understood. Rainwater infiltration considerably influences HMs concentrations in soil [12], leading to their migration and subsequent accumulation in groundwater, which in turn severely compromises groundwater quality and poses severe human health problems [13]. The transport and transformation of HMs in subsurface environments mainly depend on the characteristics and structure of soil and aquifer media, as well as the concentration and nature of HMs [14, 15]. However, the complete characterization of metal fate and transport, particularly regarding adsorption-desorption processes and relevant physical processes in soil, remains elusive. Predicting the transport and transformation of HMs in the soil, particularly their mobility and retention, is difficult. Therefore, the mechanisms governing the transport and transformation of HMs, along with their adsorption-desorption characteristics in soil-groundwater systems, remain unclear.

The infiltration of pollutants and their subsequent transformations are pivotal aspects of soil and groundwater pollution prevention and groundwater environment research. The application of numerical modeling in mitigating groundwater pollution has been extensively investigated [16−18]. Computer models have become indispensable tools for evaluating chemical changes and predicting behavioral changes in groundwater under various geochemical and hydrogeological conditions [19]. Rigorous geochemical modeling, coupled with hydrological modeling, is essential for simulating and predicting soil-groundwater contaminant transport [20]. Researchers have combined soil-water movement simulation software with groundwater simulation software to establish a coupled model of soil-groundwater movement [21, 22]. Employing the finite difference method, a three-dimensional coupled saturated-unsaturated water motion and solute transport model was developed to effectively simulate site-scale water motion and solute transport [23]. GIRAUD et al [24] established a three-dimensional numerical model to simulate polluted water quality. While RAMASAMY et al [25] employed numerical simulations to predict acid

mine drainage from acid mine wastewater. One-dimensional reactive transport modeling using PHREEQC has proven effective in simulating the transport of HMs contamination in groundwater and determining associated chemical changes (mainly arsenic contamination) within a predicted area [26]. An array of groundwater contamination risk assessment methods is available. However, these methods suffer from subjectivity, lack of validity, and an inadequate reflection of contaminant fate and groundwater contamination dynamics [27]. While process-based modeling overcomes many limitations of the exponential approach, but it is limited by the availability of robust geologic and geochemical databases and the inherent uncertainty in results. Groundwater issues of both fundamental and practical importance in inhomogeneous media, such as multiscale problems, long-term water contamination predictions, large-scale water resource assessment, ground subsidence, nonlinear (e. g., diving) challenges, and nonisothermal multiphase flow complexities [28, 29], often involve complex or large-scale conditions that incur high computational costs. Hence, quantitative evaluations rely on groundwater flow and contaminant transport modeling to determine the risk of heavy metal contamination in groundwater. Process-based models are increasingly emerging to reliably simulate and predict groundwater contamination risks under different hydrogeological and climate change conditions [30]. However, the majority of these models focus on the advection and dispersion of pollutants without considering physical, chemical, and biological processes. Moreover, only a few studies have evaluated numerical models that encompass saturated and unsaturated conditions alongside seepage zones and aquifers. Therefore, mathematically accurate and physically applicable numerical methods are needed to address these problems [31]. Despite considerable recent advancements in computational algorithms and computer hardware, challenges remain for conducting large-scale and long-term predictive simulations under complex conditions in inhomogeneous porous media [32].

FEFLOW finite element numerical simulation is widely used for the numerical modeling of groundwater contamination owing to their high simulation efficiency and capability to yield highly accurate and intuitive simulation results [33]. FEFLOW software, which operates based on the control equations of variable saturation, enables fully three-dimensional saturated-unsaturated numerical simulations. However, much of the existing research applies FEFLOW to saturated zones [34]. To accurately characterize contaminant migration patterns within the soil-groundwater system of a real site and reveal the parameter sensitivity of solute migration models, this study focuses on a contaminated site from nonferrous metal smelting (lead and zinc) in Henan Province, China. Field and laboratory experiments are combined to establish a comprehensive, three-dimensional soil-groundwater flow and solute transport model using FEFLOW software. This model incorporates convection, dispersion, adsorption, and chemical reactions into solute transport modeling. Furthermore, computational analysis, based on sensitivity analysis of the model, is conducted to reasonably reflect the migration and transformation processes of HMs pollutants within the soil-groundwater system. Through the simulation and prediction of the pollutant migration process, this study offers a theoretical basis and practical support for pollution management.

2 Materials and methods

2.1 Overview of the study area

2.1.1 Study area

This study is conducted in an abandoned zinc smelter area characterized by an average annual temperature of 12.1−15.1 ℃, an average annual precipitation of 688.6－988.3 mm, and an evaporation of 934.2 mm. Groundwater in the region flows from northeast to southwest under slight pressure, originating from the mountains and eventually reaching downstream areas before discharging into the Donggou River. The southern downstream section of the parcel is adjacent to the Donggou River, a tributary of the Yi River.

2.1.2 Geophysical exploration method

The complex geological structure of the study area is clarified according to the guidelines outlined in the Technical Regulations of Resistivity Profiling Method (DZ/T0073—2016) and Technical Regulations of Geological Radar Exploration in Hydropower Engineering (NB/T 10133—2019).

This analysis integrates high-density electrical methods and geological radar measurements based on high-frequency electromagnetic wave theory. The study area comprises nine high-density survey lines and sixteen geodetic radar sidings (Figure S1). Additionally, several boreholes are present in the area, facilitating comparison and verification. By comparing the results of the high-density electrical method with drill core findings, the main stratigraphic layers are identified and arranged from top to bottom as miscellaneous fill, silty fill, transition layer, pebble-gravel layer, and bedrock. Furthermore, the subsurface wall of the study area is inferred and identified (Figure 1(a)). The georadar profiles reveal main anomalies, such as nonpressure-bearing zones, suspected walls, and water-rich layers (Figure 1(b)).

2.1.3 Site-distribution characteristics of HMs

The descriptive statistics of toxic elements in soil samples are shown in Figure 2. In this model, soil HMs concentrations are set as mg/L, necessitating a conversion from mg/kg. To achieve this, we multiplied the HMs contamination concentration by the average density of the soil, typically 2.65 g/cm^3, which is commonly observed in mineralized soils. The screening values of Cd, Zn, Pb and As for the second category of land use were determined based on the risk screening value for soil contamination of development land (GB 36600—2018) and the U. S. Superfund Soil Screening Guidelines, with reference values set at 65, 4200, 800 and 60 mg/kg, respectively. Analysis

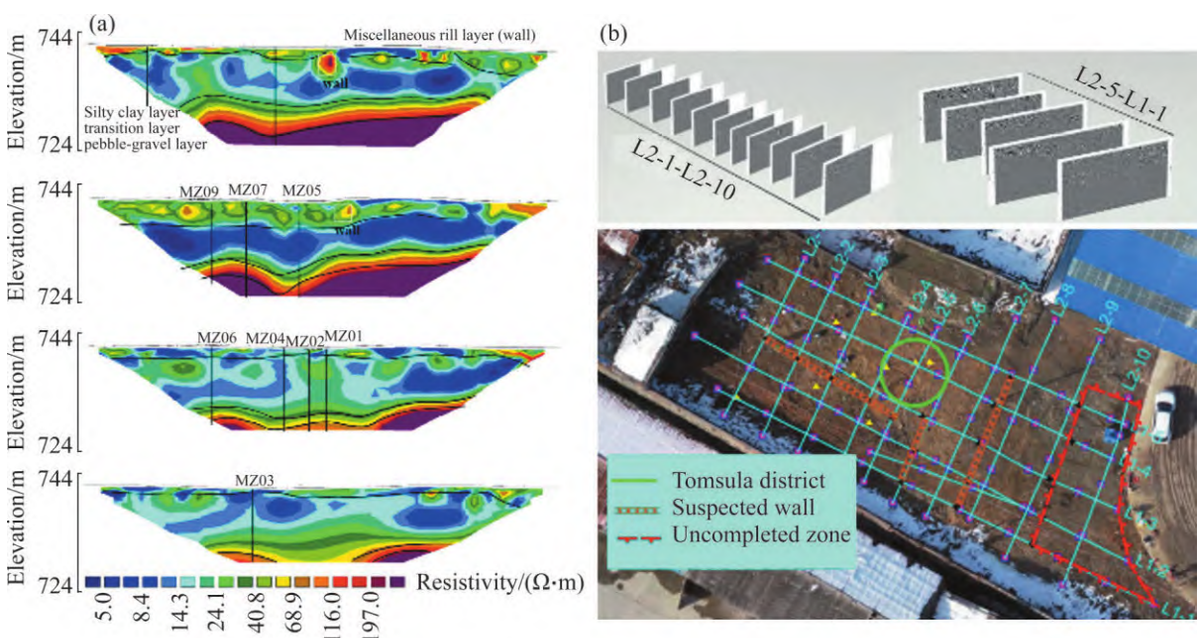

Figure 1 Interpretation results from high-density electrical method detection (a) and integrated georadar interpretation map (b)

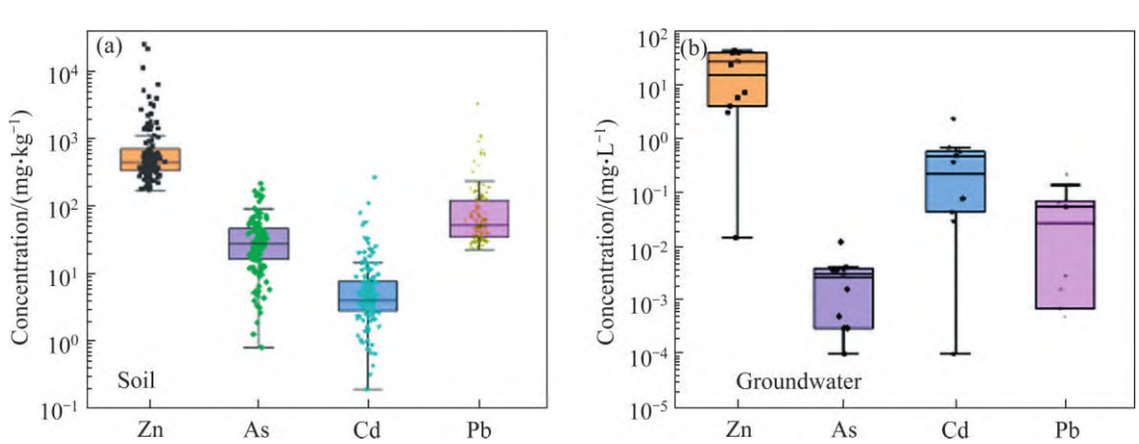

Figure 2 Box plot showing concentrations of Zn, As, Cd and Pb in soil samples (a) and groundwater (b) contamination

of surface soil samples (0−1.5 m) revealed concentrations exceeding reference values for Cd, Zn, Pb and As by 5%, 20%, 5% and 35%, respectively. This proportion decreased gradually with increasing stratigraphic depth. The pH values of the highly deep samples were mostly 3 − 4, indicating severe soil acidification in the area. Overall, HMs contamination in the soil at the smelting site is highly non-uniform and extremely serious, with many samples showing very high concentrations of HMs and overall elevated contamination levels. This situation poses a high environmental risk to the surrounding area.

In Figure 2, groundwater pH values ranged in 3.30 − 6.14, with an average of 4.72. According to the Chinese Groundwater Quality Standard (GB/T14848—2017), Class V groundwater is characterized by pH values below 5.5 or above 9.0. Monitoring well data indicated a pH exceedance rate of 70%. The standard limits for Cd, Zn, Pb and As in Chinese groundwater class V (GB/T14848—2017) are 0.01, 5.0, 0.10 and 0.05 mg/L, respectively. The contamination exceedance rates for groundwater samples followed this order: Cd (100%)>Zn (90%)>Pb (20%)>As (0).

Analyzing the spatial distribution of HM pollution in the soil is crucial for understanding pollutant migration patterns. Figure 3 shows the three-dimensional spatial distribution of HM pollution in the soil at the smelting site, established through kriging interpolation using soil and groundwater pollution data from the smelting site. Cd, Zn, Pb, and As in shallow soil exceeded the standard, and the spatial distribution of the pollution was considerably dispersed, which was attributed to smelting activities. Pollution concentrations were mainly concentrated in shallow soil and exhibited uneven horizontal and vertical distributions. In addition, the pollution of Cd, Zn, and Pb tended to spread into the surrounding space. Studies on smelting activities have found substantial changes in soil pH, with low pH greatly increasing the mobility and effectiveness of HMs (samples) [34]. Cd, Pb and Zn exhibit extremely high geochemical mobility in acidic soils, posing serious threats to neighboring ecosystems. Therefore, conducting numerical simulations of the release and adsorption processes of HMs from soil to groundwater is essential for predicting HMs pollution trends and comprehensively evaluating its risk to the surrounding environment.

2.2 Transport modeling

2.2.1 Conceptualization of regional hydrogeological conditions

As the study area is not a complete hydrogeological unit, it covers an area of ~673 m^2. The boundary around the study area serves as the model boundary, categorized as the first type of boundary, with groundwater levels on the boundary obtained through field measurements. The estimated total depth of the model is 10 m, with the vertical upward section of the model divided into four layers. The first layer comprises an artificial miscellaneous fill layer, followed by a pulverized clay layer, a pebble-gravel layer serving as the main aquifer for this simulation, and finally, a marble layer acting as a relative water-insulating substrate. Groundwater in this area is mainly recharged through rainfall and lateral surface water, flowing northeast-southwest toward the Donggou River. On-site pumping and dispersion tests yield aquifer

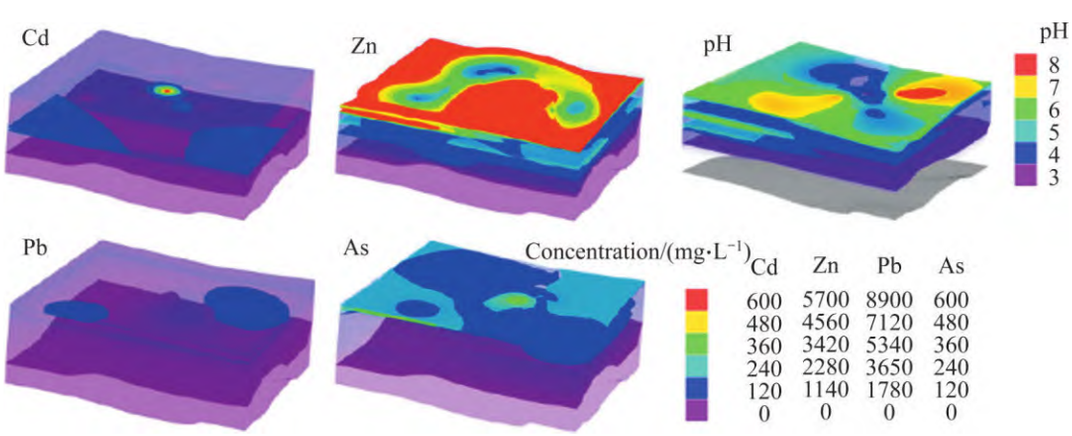

Figure 3 Spatial distribution of Pb, Zn, As, and Cd in the soil-groundwater system at the site

permeability and dispersion coefficients, supporting data for model simulations, and detailed information available in the supporting information. Constructing a three-dimensional groundwater numerical model focuses on coupled saturated and unsaturated zone processes within the soil-groundwater system. Controlling hydraulic flow equations, with head as the main variable, the governing equations for water flow in three-dimensional variably saturated porous media are shown in the support information.

2.2.2 Conceptualization of HMs transport processes

Soil and groundwater systems form an integral entity, with soil-water and groundwater systems divided into unsaturated and saturated zones, which are interconnected through groundwater flow cycles and reactive solute transport. After the HMs pollution of soil from nonferrous smelting activities, pollutants leach from the soil into groundwater along with the water flow during surface runoff and atmospheric precipitation infiltration, contaminating the groundwater. Simultaneously, HMs pollutants in groundwater undergo adsorption onto the soil during migration. Figure 4 shows the conceptual model of HMs transport and diffusion in soil and groundwater. In multispecies migration, heterogeneous reactions (i. e., interactions between species in fluid and solid phases) depict the transformation process of pollutants through reaction coefficients (λ). These reaction coefficients (λ) and retention coefficients (R) express the release of different HMs from soil to groundwater and the ability of the soil to adsorb HMs from groundwater. Solute transport encompasses convective, dispersive, adsorptive, and reactive processes. Reaction and retention coefficients are determined from soil HMs concentration data collected during site investigation, serving as the initial conditions for the simulation, while groundwater HMs contamination data are used as reference values. Under the solute transport section, reactive solute transport is considered, focusing mainly on the effects of reaction coefficients (λ) and retention coefficients (R) on solute transport. The controlling equations for groundwater flow and solute transport are shown in the supporting information.

2.2.3 Model parameterization and identification validation

Based on the hydrogeological conditions, the study area was generalized into a nonhomogeneous, anisotropic, three-dimensional, unsteady seepage system. The soil parameters were obtained from soil tests and relevant literature, while aquifer hydrogeological parameters were mainly sourced from previous hydrogeological investigations. Solute transport encompasses convection, dispersion, adsorption, and reaction processes. The dispersion coefficient, influenced by soil nature, was obtained through experiments and a literature review. Longitudinal dispersion is the ratio of the dispersion coefficient to the average pore water flow rate, and the transverse dispersion is 1/5 of the longitudinal dispersion. λ and k were determined using soil HMs concentration data obtained from site investigations as the initial condition for simulation, while groundwater HMs contamination data served as the reference value.

The “trial-and-error method” is mainly used for adjustment. Initially, the model incorporates the initial values of the parameters within the study area, yielding the initial flow field. Subsequently, after calculating steady flow, adjustments are made

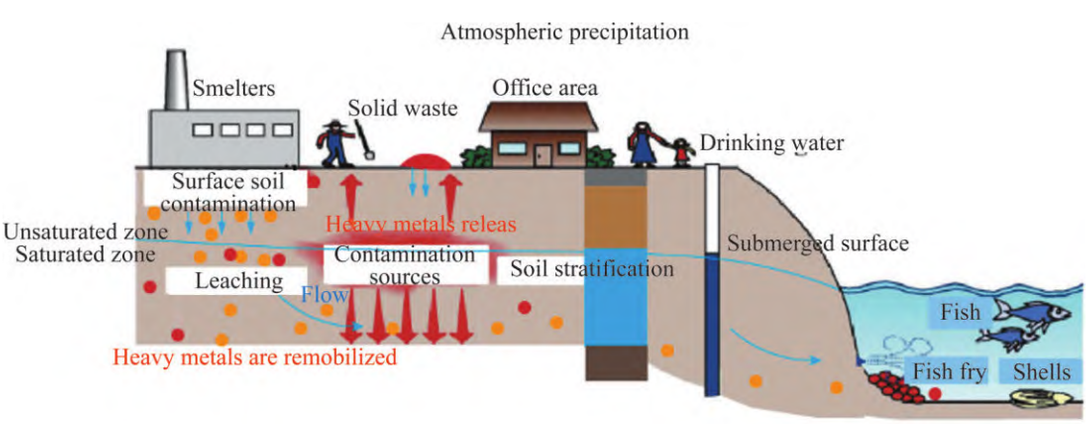

Figure 4 The conceptual model of heavy metal transport and diffusion in soil and groundwater

to the parameters of the natural flow field based on actual observed water levels. The corrected initial groundwater flow field shows that the initial flow field of the model aligns closely with the actual hydrogeological conditions of the study area, reflecting the characteristics of the actual flow field. Table S1 outlines the reactive solute transport parameters. Therefore, the flow field obtained from the model serves as the initial flow field for unsteady flow and forms the basis for solute transport simulation.

3 Result and discussion

3.1 Pollution prediction results

Groundwater contamination and soil contamination are somewhat consistent. The established groundwater flow and solute transport models were used for the predictive analysis of contaminant migration. Reaction and retention coefficients were used to characterize the transport of different HMs in groundwater. The concentrations of HMs pollutants Cd, Zn, Pb and As at corresponding depths of soil samples tested in the study area in March 2023 served as their initial concentrations, with pollutant concentrations in groundwater serving as reference values. Figure 5 illustrates the modeled and predicted spatial and temporal trends of HMs contaminants in soil and groundwater at day 1737.98, 4829.46 and 10000.

According to the model simulation results, pollution is continuously released into the groundwater, and the degree of groundwater pollution is closely related to soil pollution. The highest value of Cd pollution halo center concentration in the upper soil reached 600 mg/L, but over time, the initial soil pollution halo showed a decreasing trend, while groundwater pollution steadily increased to 1.6 mg/L, resulting in groundwater Cd pollution exceeding the standard. Similarly, high level of Zn contamination in soil translates into groundwater contamination exceeding 100 mg/L. Conversely, as soil contamination of Cd is less severe, it continues to

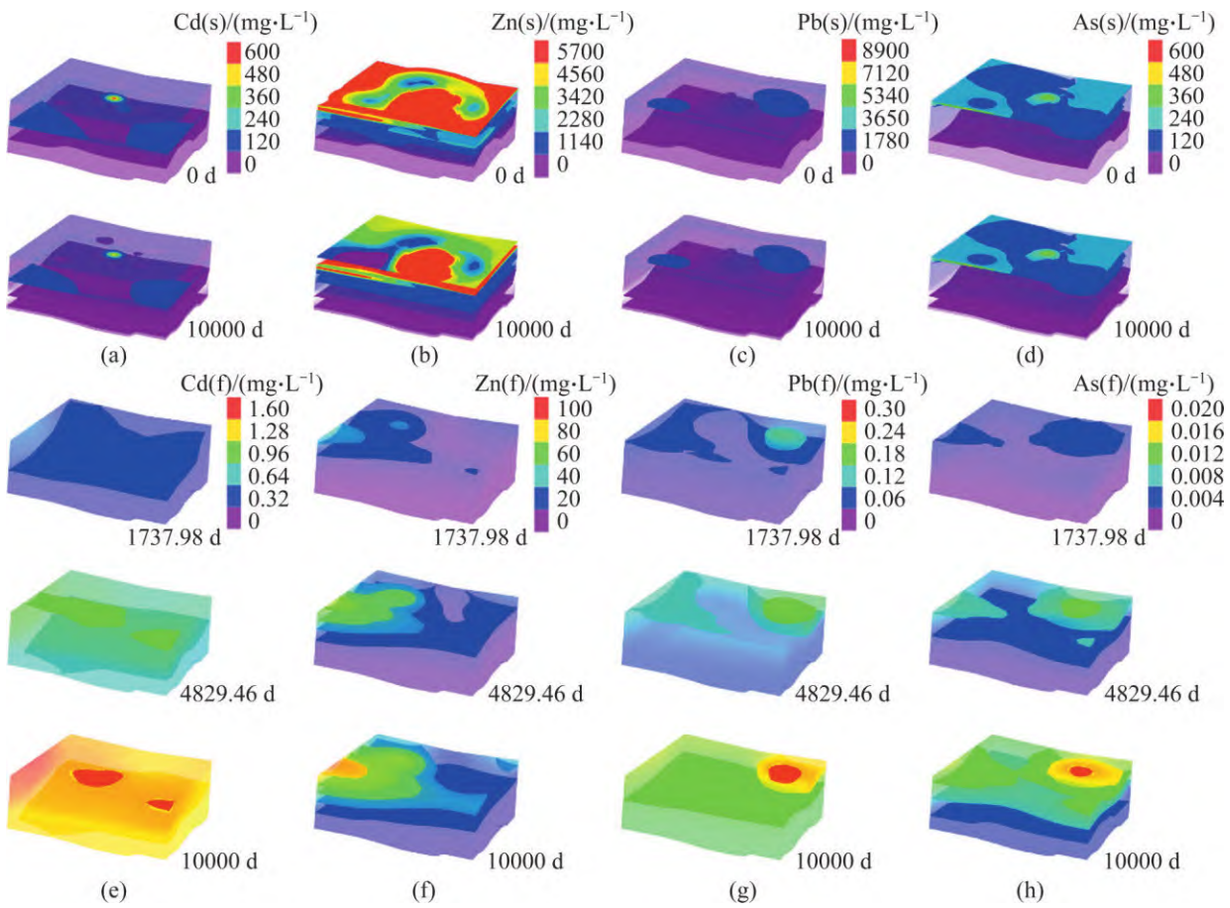

Figure 5 Spatial and temporal trends in the modeling of transport diffusion of Cd (a, e), Zn (b, f), Pb (c, g) and As (d, h) heavy metal contaminants in soil (a, b, c, d) and groundwater (e, f, g, h)

leach into the groundwater during the simulation process, resulting in less serious Pb contamination in groundwater. Throughout the simulation, As pollution in soil remains considerably stable, with groundwater As content remaining below the standard threshold. Geophysical exploration and well drilling results indicate the complex underground geological conditions of the site owing to its historical legacy, which influences pollutant transportation. This complex subsurface environment leads to complex local mobility of the groundwater flow field, causing HMs migration in soil groundwater to deviate somewhat from the direction of groundwater flow at the site. However, the overall migration direction remains consistent with the direction of groundwater at the site.

Combining the simulation prediction results with the analysis of groundwater HMs contamination, it was determined that the mobility of different HMs released from soil to groundwater follows the sequence: Cd>Zn>Pb>As. Notably, the retention coefficient of As was larger than that of Cd, Zn and Pb. The simulation results showed the continuous release of pollutants exceeding standards from soil to groundwater over time. The distance from the source is closely related to the concentration of HMs contaminants in the groundwater. Meanwhile, the maximum migration distance of pollutants increases with time, albeit at a decreasing rate, resulting in low pollutant concentrations. The highly heterogeneous nature of soil and groundwater contamination at contaminated sites, coupled with the unpredictability and hidden nature of underground spaces, pose challenges in comprehensively understanding of heavy metal transport and transformation processes in soil and groundwater.

3.2 Sensitivity analysis

Soil is an important medium for groundwater contamination, with contaminants mainly infiltrating the ground from soil and contaminating groundwater through atmospheric precipitation, surface water, or the infiltration and leaching of irrigation water. To simplify the solute transport model, the concentration of Zn in the soil was selected as the initial pollutant concentration for simulation and parameter sensitivity analysis. During the simulation of Zn transport in soil and groundwater, a reaction coefficient of 1×10^{-5} s^{-1} and a retention coefficient of 1 were utilized. The values of these coefficients were altered to study their effect on pollutant transport.

Figure 6(a) illustrates a noticeable change in the curve when the retention coefficient differs by one order of magnitude. This alteration results in a notable slowdown in pollutant transport and a decrease in pollutant concentration at the same observation point. Specifically, the retention coefficient was adjusted to a response factor of 1×10^{-4} s^{-1}. When the model was simulated for 3626 days with retardation coefficients of 0.1, 1 and 10, the zinc concentrations at the observation points were 1041.47 mg/L, 326.93 mg/L and 20.25 mg/L respectively. Over a simulation period of 3626 d, altering the retention coefficient from 0.1 to 1 led to

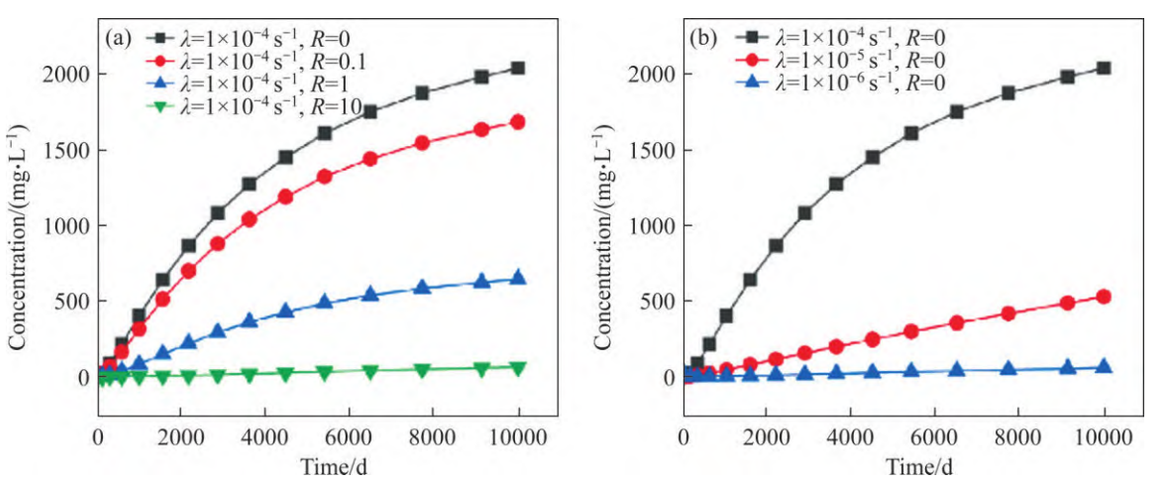

Figure 6 Parametric sensitivity analysis of (a) retention coefficients (R) and (b) reaction coefficients (λ) during heavy metal transport and diffusion in soil groundwater using Zn as an example

an average decrease of 68% in the Zn concentration at the observation points. Similarly, Zn concentration decreased by an average of 93% at the observation point when the retention coefficient was changed from 1 to 10. The magnitude of the retention coefficient characterizes the strength of the adsorption capacity of soil particles to pollutants, with large retention coefficients implying enhanced soil adsorption of pollutants and slow pollutant migration. The effect of the retention coefficient on pollutant transport may be attributed to the presence of clayey soil in the study area, characterized by highly dispersed particles with uneven charges and large surface energy for adsorbing HMs in water [35].

As shown in Figure 6(b), a substantial change occurs in the curve when the reaction constant decreases by one order of magnitude. This alteration results in a notable slowdown in the rate of pollutant transport and a substantial decrease in pollutant concentration at the same distance. When the adsorption constant is 0, the reaction coefficient changes. In a model simulation lasting 3626 d, the reaction coefficients were 0.0001, 0.00001 and 0.000001, respectively, with corresponding zinc concentrations at observation points of 1274.90 mg/L, 199.72 mg/L and 21.00 mg/L. During the 3626-day simulation, as the reaction coefficient changed from 1×10^{-4} s^{-1} to 1×10^{-5} s^{-1}, the average decrease in zinc concentration at the observation point was 85%. Similarly, when the reaction coefficient changed from 1×10^{-5} s^{-1} to 1×10^{-6} s^{-1}, the average decrease in zinc concentration at the observation point was 89%. Taking As in the study area as an example, acidic soil exhibits strong immobilization of As, making it challenging for As to be released into the groundwater. Even if a small number of pollutants run off with water, they will be immobilized by the soil in other areas. In contrast, the fixation capacity of acidic soil for Cd is much smaller than that for As, resulting in Cd being easily released from the soil. Additionally, the adsorption capacity of the soil for Cd is weaker compared to As, leading to severe Cd pollution in groundwater. Throughout the process of HMs release and migration in soil-groundwater, the reaction coefficient is closely related to the retention coefficients and the physicochemical properties of the soil. It is often difficult to separate the effects of the blocking coefficients and the reaction constants in simulations at extended time scales.

3.3 Model simulation of soil remediation technologies

Regarding remediation technology for HMs pollution at smelting sites, the main method for soil HM pollution remediation at smelting sites currently entails solidification/stabilization technology, including both in situ and ex situ remediation approaches. Simulation of solidification and stabilization technology smelting site involves modifying the reaction coefficient during the release and diffusion of HMs in soil groundwater. Additionally, permeable reactive barriers (PRBs) serve as an effective means to manage groundwater pollution, with successful remediation cases documented. PRBs achieve pollution interception by building a permeable wall along the migration path of groundwater pollution plumes. Through precipitation, adsorption, oxidation-reduction, and other reactions between the reaction wall filler and the pollutants, PRBs effectively mitigate groundwater contamination.

The effects of remediation technologies on the spatial distribution of HMs contamination in soil and groundwater were analyzed by simulating the remediation effects of agents with different remediation capacities on surface-contaminated soils using zinc concentration in site soils as the initial contaminant (Figure 7(a)). Figures 8(a) and (b) show simulation results of observation points near and far from the pollutant source under the remediation conditions of remediation agents under different remediation capacities. The natural release capacity of Zn from the soil, represented by a reaction coefficient of 1×10^{-5} s^{-1}, is established. On day 2081, the Zn concentration at the observation point near the pollution source without remediation was 42.84 mg/L. When the remediation agent possessed reaction coefficients of 1×10^{-6}, 1×10^{-7} and 1×10^{-8} s^{-1}, the Zn concentration reduced by 83%, 92.01% and 92.88%, respectively. Meanwhile, the concentration of heavy metals at observation points distant from the pollution source decreased from 1.13 mg/L (untreated) to 0.90, 0.88 and 0.88 mg/L with increasing remediation agent capacities at

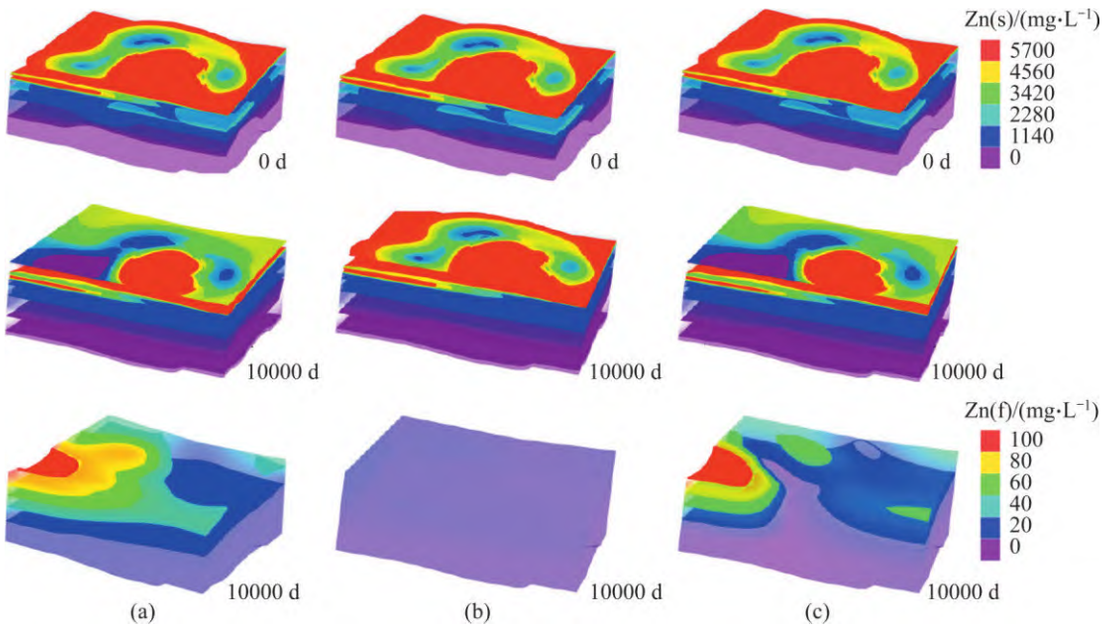

Figure 7 (a) Simulation results of Zn migration and diffusion in soil groundwater at the site before remediation; (b) Simulation results of the soil solidification and stabilization technology at the smelting site; (c) Simulation results of permeable reactive wall groundwater remediation technology

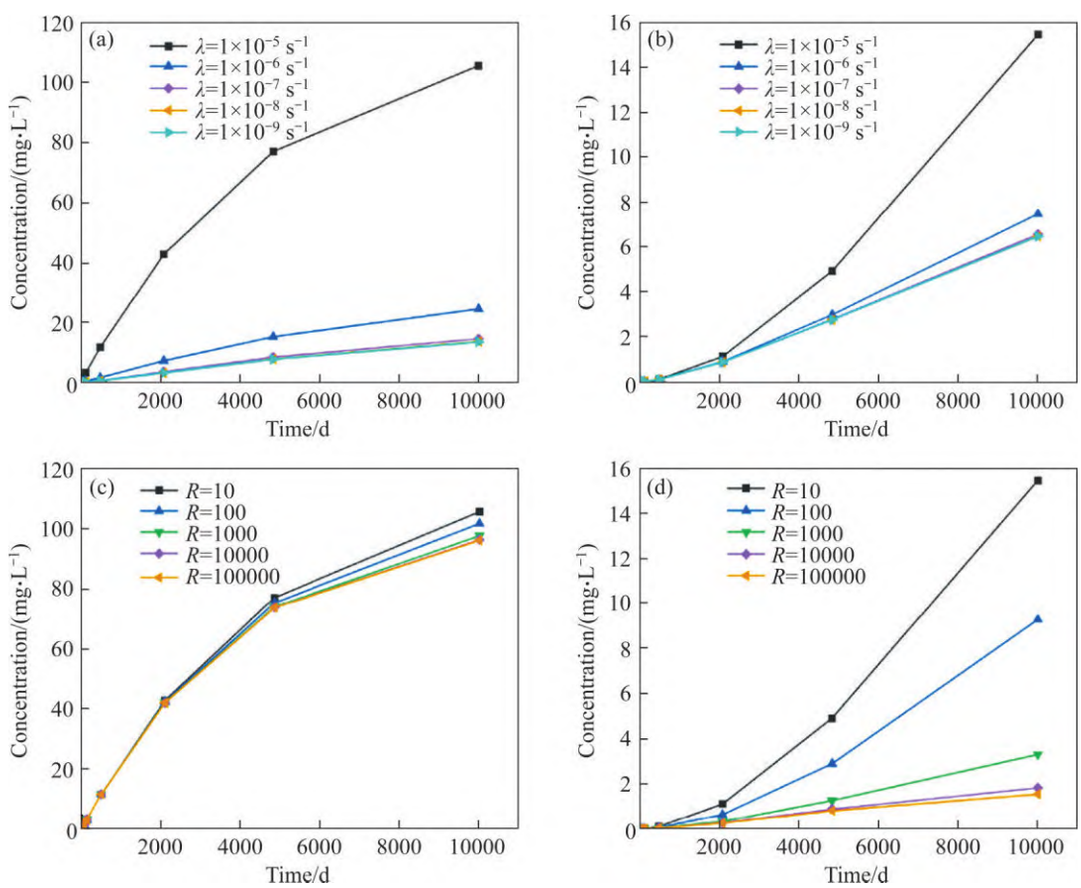

Figure 8 Zn contamination of groundwater assessed at observation sites both before and after remediation, including treatments with remediation chemicals and permeable reactive walls with varying capabilities: (a, b) Zn concentrations near and far from the pollution source when soil solidification stabilization technology is implemented at the smelting site; (c, d) Zn concentrations near and far from the pollution source when permeable reactive wall groundwater remediation technology is applied at the same site

1×10^{-6}, 1×10^{-7}, and 1×10^{-8} s^{-1}, respectively.

Figure 7(b) illustrates the treatment effects simulated through infiltration reaction walls with different remediation capacities in remediating heavily contaminated groundwater, using zinc concentration in the site soil as the initial contaminant. Figures 8(c) and (d) show simulation results of observation points located near and far from the contamination source under PRBs remediation conditions with different remediation capacities, where R of 10 is the adsorption capacity of soil for Zn under the natural condition. Throughout the simulation period, PRBs had minimal effect on reducing Zn concentration at observation points close to the pollution source. This is attributed to the high concentrations of HMs present in all the surface layers of the soil at the site. Moreover, since the observation point is situated at a distance from PRBs, contaminated groundwater that has not encountered PRBs remains downstream of the PRBs, potentially mixing with the clean water after remediation and leading to continued groundwater contamination.

3.4 Diffusive flux calculation of HMs before and after remediation

Figures 9(a)−(d) depict the results of calculating the boundary pollutant diffusion flux during the soil solidification and stabilization remediation process by placing the boundary downstream of the study area. At simulation time day 6538, the diffusion flux at the boundary without treatment is 54.18 mg/(d·m^2). With repair agents of λ values 5×10^{-6} s^{-1}, 1×10^{-6} s^{-1} and 5×10^{-7} s^{-1}, the diffusion fluxes at the boundary decrease to 20.02, 16.12 and 15.73 mg/(d·m^2), respectively. By day 6538, the cumulative diffusion fluxes at the boundary are 195496.08, 69108.47, 55332.73 and 53944.00 mg/m^2, with reduction rates of 64.64%, 71.69% and 72.40%, respectively. The percentage of diffusion flux reduction is influenced by the selection of boundary position and area. The model simulation results effectively illustrate the remediation technology principle. In areas near the pollution source, treatment activities lead to a decrease in heavy metal release into groundwater, while in distant areas, heavy metal content diminishes.

Figures 9(e)−(h) show the results of setting a boundary within the study area and downstream of the PRBs, calculating the diffusion fluxes of contaminants. By day 6538 of stimulation, the diffusive flux at the selected boundary without remediation was 54.18 mg/(d·m^2), which was reduced to 10.64, 0.03 and 0 mg/(d·m^2) when the retention coefficients of PRB were 50, 100 and 1000, and the corresponding reductions in diffusive fluxes were 80.35%, 99.95% and 100%, respectively. Up to day 6538, the cumulative diffusive fluxes at the boundary were 195496.08, 26273.28, 63.14 and 0.12 mg/m^2, respectively, further indicating the substantial reduction in diffusive fluxes. This reduction is attributed to the placement of the boundary behind PRB, demonstrating the effectiveness of PRBs in treating heavily contaminated groundwater.

4 Conclusions

1) The hydrogeological conditions and pollution distribution in the study area are complex owing to historical legacy problems. The combined use of geophysical exploration techniques, such as the georadar method and high-density electrical resistance method, along with borehole exploration, helps to characterize HMs contamination at the site in detail. This provides important support for establishing and studying the model. Smelting activities considerably influence the distribution of HMs contamination at the site. Different HMs exhibit varying migratory capacities and depths of influence, with Cd>Zn>Pb>As under acidic conditions. The construction of a process-based reactive solute transport model of HMs in soil groundwater is crucial for predicting HMs pollution trends and comprehensively evaluating their risks to the surrounding environment.

2) The constructed reactive solute migration model aligns with the actual site conditions. It was determined that under the action of reaction and retention coefficients, the release and migration capacities of different HMs from soil to groundwater followed the order: Cd>Zn>Pb>As, among which the adsorption capacity of As was larger than that of Cd, Zn and Pb. In the process of release and migration of HMs in soil and groundwater, the reaction and retention coefficients

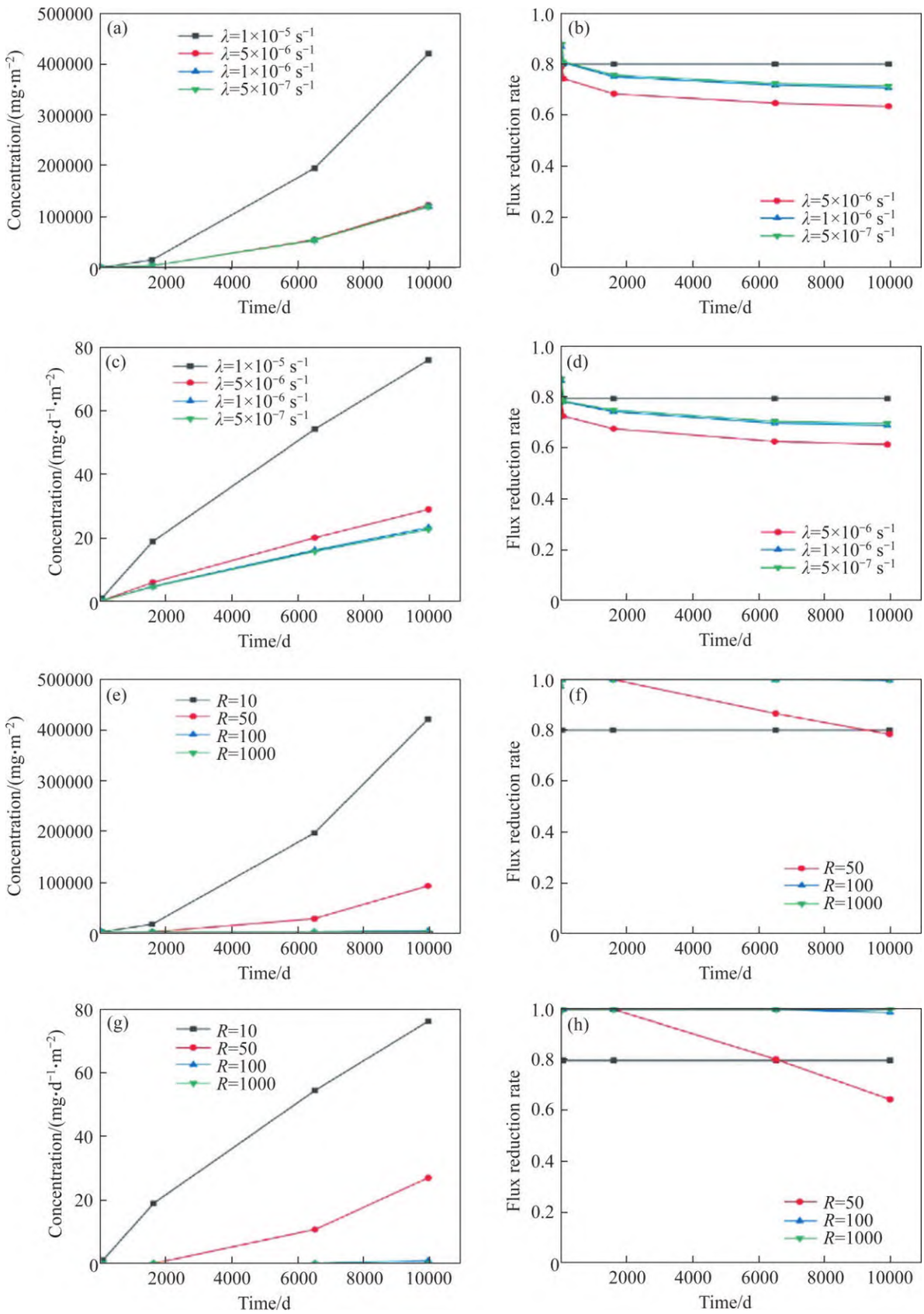

Figure 9 Changes in boundary diffusive fluxes (a) and reduction rates (b) after soil remediation; Daily changes of diffusive fluxes (c) and reduction rate (d) of boundary diffusion flux after soil remediation; Changes in boundary diffusive fluxes (e) and reduction rates (f) after groundwater remediation; Daily changes of boundary diffusive fluxes (g) and reduction rates (h) after groundwater remediation

are closely related to the retention coefficients and physicochemical properties of the soil. Hence, separating the effects of reaction and retention coefficients in extended simulations can be challenging.

3) Based on comprehensive site contamination characteristics, hydrogeological conditions, and environmental hazard analysis, a synergistic approach to remediating soil-groundwater HMs contamination at smelting sites has been proposed. This approach includes soil solidification and stabilization remediation technology and PRB sremediation technology. The model simulation results effectively illustrate the principle of the remediation technology: in the area close to the contamination source, the number of HMs released into groundwater is high owing to the treatment activities, while far from the contamination source, the HMs content decreases. Reaction coefficients of 1×10^{-7} and 1×10^{-8} showed no evident changes in the effectiveness of remediation treatment, highlighting the importance of selecting appropriate remediation materials. As the boundary is selected behind PRBs, there is a notable reduction in the diffusion flux of contaminants, indicating the effectiveness of PRBs in treating localized, heavily polluted groundwater. The constructed reactive solute transport model simulates the treatment effects of different remediation technologies and synergistic soil-groundwater treatment, providing guidance for soil-groundwater remediation technologies.

Supplementary materials

http://qr.csupress.com.cn/Public/ResourceList/Detail/51404
Please scan the QR code or visit the URL link to get the supporting information

Contributors

ZHANG Hai-li performed experiments and modeling and wrote the first draft of the manuscript. ZHAO Peng, GAO Wen-yan, YANG Xue-feng, SONG Lei, SUN Jing and XIAO Bao-hua formulated the overall research objectives, supported the acquisition of funding, and edited the first draft of the manuscript. FENG Xiang, GUO Lin, LU Yong-ping, LI Hai-feng provided site support. GUO Lin, LU Yong-ping and LI Hai-feng provided research site support. All authors participated in responding to reviewers' comments and revised the final version.

Conflict of interest

ZHANG Hai-li, ZHAO Peng, GAO Wen-yan, XIAO Bao-hua, YANG Xue-feng, SONG Lei, FENG Xiang, GUO Lin, LU Yong-ping, LI Hai-feng and SUN Jing declare that they have no conflict of interest.

References

[1] ADNAN M, XIAO Bao-hua, XIAO Pei-wen, et al. Research progress on heavy metals pollution in the soil of smelting sites in China [J]. Toxics, 2022, 10(5): 231. DOI: 10.3390/toxics10050231.

[2] EL-AASSAR A H, HAGAGG K, HUSSIEN R, et al. Integration of groundwater vulnerability with contaminants transport modeling in unsaturated zone, case study El-Sharqia, Egypt [J]. Environmental Monitoring and Assessment, 2023, 195(6): 722. DOI: 10.1007/s10661-023-11298-3.

[3] MA Jun-hua, SINGHIRUNNUSORN W. Distribution and health risk assessment of heavy metals in surface dusts of maha sarakham municipality [J]. Procedia − Social and Behavioral Sciences, 2012, 50: 280 − 293. DOI: 10.1016/j.sbspro.2012.08.034.

[4] JIANG Zhi-chao, GUO Zhao-hui, PENG Chi, et al. Heavy metals in soils around non-ferrous smelteries in China: Status, health risks and control measures [J]. Environmental Pollution, 2021, 282: 117038. DOI: 10.1016/j. envpol. 2021. 117038.

[5] LI Chang-feng, ZHOU Ke-hai, QIN Wen-qiang, et al. A review on heavy metals contamination in soil: Effects, sources, and remediation techniques [J]. Soil and Sediment Contamination, 2019, 28(4): 380−394. DOI: 10.1080/15320383.2019.1592108.

[6] HE Zhen-li, SHENTU J, YANG Xiao-e, et al. Heavy metal contamination of soils: Sources, indicators and assessment [J]. Journal of Environmental Indicators, 2015, 9: 17−18.

[7] YUE Lin, GE Cheng-jun, FENG Dan, et al. Adsorption-desorption behavior of atrazine on agricultural soils in China [J]. Journal of Environmental Sciences, 2017, 57: 180−189. DOI: 10.1016/j.jes.2016.11.002.

[8] SERRANO S, GARRIDO F, CAMPBELL C G, et al. Competitive sorption of cadmium and lead in acid soils of Central Spain [J]. Geoderma, 2005, 124(1−2): 91−104. DOI: 10.1016/j.geoderma.2004.04.002.

[9] ARCO-LÁZARO E, AGUDO I, CLEMENTE R, et al.

Arsenic(V) adsorption-desorption in agricultural and mine soils: Effects of organic matter addition and phosphate competition [J]. Environmental Pollution, 2016, 216: 71−79. DOI: 10.1016/j.envpol.2016.05.054.

[10] ZHAO X, JIANG T, DU B. Effect of organic matter and calcium carbonate on behaviors of cadmium adsorption-desorption on/from purple paddy soils [J]. Chemosphere, 2014, 99: 41−48.

[11] JING Feng, CHEN Xiao-min, YANG Zhi-jiang, et al. Heavy metals status, transport mechanisms, sources, and factors affecting their mobility in Chinese agricultural soils [J]. Environmental Earth Sciences, 2018, 77(3): 104. DOI: 10.1007/s12665-018-7299-4.

[12] ZIMMERMANN J, DIERKES C, GÖBEL P, et al. Metal concentrations in soil and seepage water due to infiltration of roof runoff by long term numerical modelling [J]. Water Science and Technology: A Journal of the International Association on Water Pollution Research, 2005, 51(2): 11−19.

[13] AZIZULLAH A, KHATTAK M N K, RICHTER P, et al. Water pollution in Pakistan and its impact on public health: A review [J]. Environment International, 2011, 37(2): 479−497. DOI: 10.1016/j.envint.2010.10.007.

[14] HASHIM M A, MUKHOPADHYAY S, SAHU J N, et al. Remediation technologies for heavy metal contaminated groundwater [J]. Journal of Environmental Management, 2011, 92(10): 2355 − 2388. DOI: 10.1016/j. jenvman. 2011. 06.009.

[15] MAHAJAN M, GUPTA P K, SINGH A, et al. A comprehensive study on aquatic chemistry, health risk and remediation techniques of cadmium in groundwater [J]. Science of the Total Environment, 2022, 818: 151784. DOI: 10.1016/j.scitotenv.2021.151784.

[16] BAI Xue, SONG Kai, LIU Jian, et al. Health risk assessment of groundwater contaminated by oil pollutants based on numerical modeling [J]. International Journal of Environmental Research and Public Health, 2019, 16(18): 3245. DOI: 10.3390/ijerph16183245.

[17] MASOOD Z B, ABD ALI Z T. Numerical modeling of two-dimensional simulation of groundwater protection from lead using different sorbents in permeable barriers [J]. Environmental Engineering Research, 2020, 25(4): 605−613. DOI: 10.4491/eer.2019.237.

[18] SHAMSUDDUHA M, ZAHID A, BURGESS W G. Security of deep groundwater against arsenic contamination in the Bengal Aquifer System: A numerical modeling study in southeast Bangladesh [J]. Sustainable Water Resources Management, 2019, 5(3): 1073−1087. DOI: 10.1007/s40899-018-0275-z.

[19] CHIDAMBARAM S, ANANDHAN P, PRASANNA M V, et al. Hydrogeochemical modelling for groundwater in neyveli aquifer, Tamil Nadu, India, using PHREEQC: A case study [J]. Natural Resources Research, 2012, 21(3): 311−324. DOI: 10.1007/s11053-012-9180-6.

[20] XUE Sheng-guo, KE Wen-shun, ZENG Jia-qing, et al. Pollution prediction for heavy metals in soil-groundwater systems at smelting sites [J]. Chemical Engineering Journal, 2023, 473: 145499. DOI: 10.1016/j.cej.2023.145499.

[21] FACCHI A, ORTUANI B, MAGGI D, et al. Coupled SVAT-groundwater model for water resources simulation in irrigated alluvial Plains [J]. Environmental Modelling & Software, 2004, 19(11): 1053−1063. DOI: 10.1016/j.envsoft. 2003.11.008.

[22] NISWONGER R G, PRUDIC D E. Modeling variably saturated flow using kinematic waves in MODFLOW [M]// Groundwater Recharge in a Desert Environment: The Southwestern United States. Washington, D. C.: American Geophysical Union, 2004: 101 − 112. DOI: 10.1029/009 wsa07.

[23] YAKIREVICH A, BORISOV V, SOREK S. A quasi three-dimensional model for flow and transport in unsaturated andsaturated zones: 1. Implementation of the quasi two-dimensional case [J]. Advances in Water Resources, 1998, 21(8): 679−689.

[24] GIRAUD Q, GONÇALVÈS J, PARIS B, et al. 3D numerical modelling of a pulsed pumping process of a large DNAPL pool: In situ pilot-scale case study of hexachlorobutadiene in a keyed enclosure [J]. Journal of Contaminant Hydrology, 2018, 214: 24−38. DOI: 10.1016/j.jconhyd.2018.05.005.

[25] RAMASAMY M, POWER C, MKANDAWIRE M. Numerical prediction of the long-term evolution of acid mine drainage at a waste rock pile site remediated with an HDPE-lined cover system [J]. Journal of Contaminant Hydrology, 2018, 216: 10−26. DOI: 10.1016/j.jconhyd.2018.07.007.

[26] ASHRAF A, CHEN X, RAMAMURTHY R. Modelling heavy metals contamination in groundwater of Southern Punjab, Pakistan [J]. International Journal of Environmental Science and Technology, 2021, 18(8): 2221−2236. DOI: 10.1007/s13762-020-02965-w.

[27] COUNCIL N R, EARTH D O, STUDIES L, et al. Ground water vulnerability assessment: Predicting relative contamination potential under conditions of uncertainty [M]. Washington DC: National Academies Press, 1993.

[28] ORTIZ-ZAMORA D, ORTEGA-GUERRERO A. Evolution of long-term land subsidence near Mexico City: Review, field investigations, and predictive simulations [J]. Water Resources Research, 2010, 46(1): W01513. DOI: 10.1029/2008wr007398.

[29] TSAKIROGLOU C D. A multi-scale approach to model two-phase flow in heterogeneous porous media [J]. Transport in Porous Media, 2012, 94(2): 525−536. DOI: 10.1007/s11242-011-9882-y.

[30] SEGE J, GHANEM M, AHMAD W, et al. Distributed data collection and web-based integration for more efficient and informative groundwater pollution risk assessment [J]. Environmental Modelling & Software, 2018, 100: 278−290. DOI: 10.1016/j.envsoft.2017.11.027.

[31] CUSHMAN J H, TARTAKOVSKY D M. The handbook of groundwater engineering [M]. Boca Raton: CRC Press, 2016. DOI: 10.1201/9781315371801.

[32] JU Yang, GONG Wen-bo, CHANG Wei, et al. Effects of pore characteristics on water-oil two-phase displacement in non-homogeneous pore structures: A pore-scale lattice Boltzmann model considering various fluid density ratios [J]. International Journal of Engineering Science, 2020, 154: 103343. DOI: 10.1016/j.ijengsci.2020.103343.

[33] LU Wei, YANG Qing-chun, MARTÍN J D, et al. Numerical modelling of seawater intrusion in Shenzhen (China) using a 3D density-dependent model including tidal effects [J].

Journal of Earth System Science, 2013, 122(2): 451－465. DOI: 10.1007/s12040-013-0273-3.

[34] SHERENE T. Mobility and transport of heavy metals in polluted soil environment [J]. Biological forum—An International Journal, 2010, 2(2): 112−121.

[35] DUBE A, ZBYTNIEWSKI R, KOWALKOWSKI T, et al. Adsorption and migration of heavy metals in soil [J]. Polish Journal of Environmental Studies, 2001, 10(1): 1−10.

(Edited by YANG Hua)

中文导读

土壤和地下水中重金属污染物迁移模型：以某有色金属冶炼厂为例

摘要：冶炼厂表层土壤重金属污染严重。由于数据采集和计算量的限制，大多数数值模拟将土壤和地下水分开，这与实际情况不符。本文以某冶炼厂为研究对象，将土壤和地下水视为一个整体系统，建立了土壤-地下水反应性溶质迁移三维耦合数值模型，以定量表征重金属在土壤和地下水中的迁移规律。模型采用反应系数(λ)和滞留系数(R)来描述重金属的释放和吸附能力。模型结果与现场实际污染分布一致，表明土壤-地下水修复技术对严重污染土壤和局部污染地下水均有良好的修复效果。所构建的土壤-地下水反应性溶质迁移三维耦合模型很好地描述和预测研究地点重金属的分布和迁移扩散行为。

关键词：有色金属冶炼场；重金属污染；迁移和转化机制；扩散通量预测；修复技术模拟